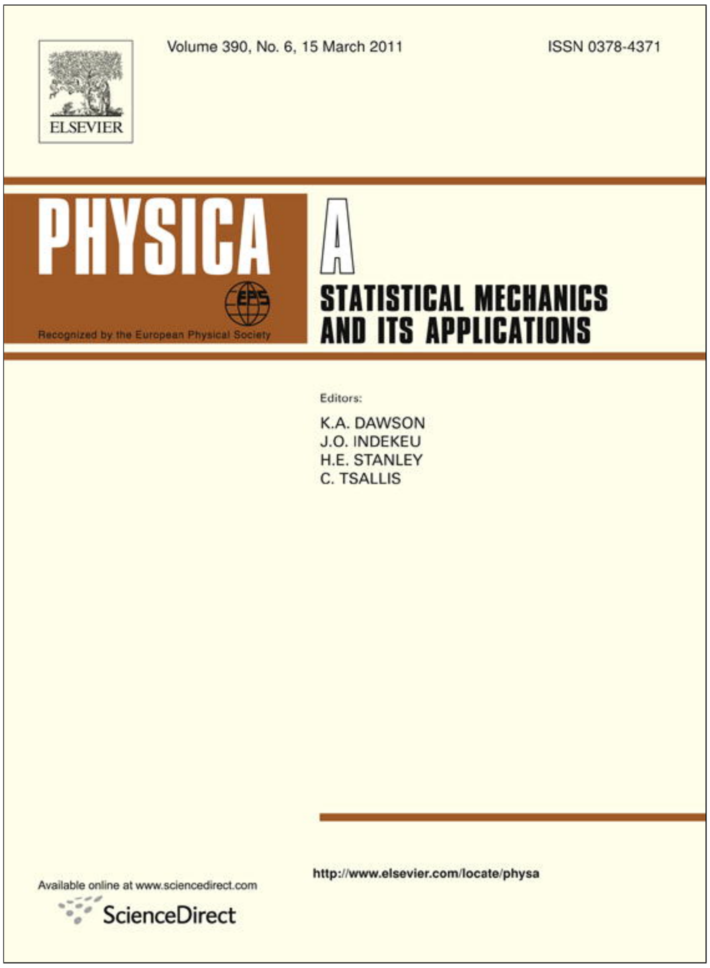
Volume 390, No. 6, 15 March 2011
ISSN 0378-4371
ELSEVIER
PHYSICA A
STATISTICAL MECHANICS AND ITS APPLICATIONS
Recognized by the European Physical Society
Editors:
K.A. DAWSON
J.O. INDEKEU
H.E. STANLEY
C. TSALLIS
http://www.elsevier.com/locate/physa
Available online at www.sciencedirect.com
ScienceDirect

Physica A 390 (2011) 1117–1123

Contents lists available at ScienceDirect

Physica A

journal homepage: www.elsevier.com/locate/physa

Coherent calcium puff signals driven by intracellular noises

Rong Sheng [a], Sten Rüdiger [b], Jianwei Shuai [c,*]

[a] Department of Computer Science, Sichuan University of Arts and Science, Dazhou, Sichuan 635000, China
[b] Institute of Physics, Humboldt-Universität zu Berlin, Germany
[c] Department of Physics and Institute of Theoretical Physics and Astrophysics, Xiamen University, Xiamen 361005, China

ARTICLE INFO

Article history:
Received 1 April 2010
Received in revised form 14 October 2010
Available online 6 December 2010

Keywords:
Intracellular signals
Calcium signals
Noise
Stochastic resonance
Coherence resonance

ABSTRACT

In many cell types, intracellular calcium is released from internal stores through calcium release channels which are distributed in clusters with a few tens of channels. Localized calcium release events, i.e. Ca^{2+} puffs, are subjected to stochastic channel dynamics and fluctuations of environmental calcium. Driven by the internal channel noise or external calcium noise, the localized calcium puffs show a coherence resonance phenomenon at weak stimulus. Our study indicates that coherent calcium puffs with an enhanced periodicity can be achieved with external calcium noise more easily than with internal channel noise.

1. Introduction

Many important cellular functions are regulated by intra- and intercellular Ca^{2+} signals. Ca^{2+} triggers life at fertilization, and controls the development and differentiation of cells into specialized types [1]. It mediates the subsequent activity of cells and is invariably involved in cell death. It is shown that the information is mainly encoded in the frequency of calcium signals. By varying the frequency of Ca^{2+} signals, different genes can be activated [2,3]. The oscillation frequency of calcium signals can then direct cells along specific developmental pathways. Furthermore, it is found that the calmodulin-dependent protein kinase II can decode the frequency of calcium oscillation into distinct levels of kinase activity [4].

Calcium ions can be released from the endoplasmic reticulum (ER), an internal store in cells with high calcium concentration, through inositol 1,4,5-triphosphate receptors (IP_3R) or Ryanodine receptors (RyR) [1]. Recent experiments have revealed that the IP_3Rs are clustered with an approximate size of hundreds of nanometers and approximately a few tens of IP_3R channels in each cluster [5,6]. The cluster distance is about 2 μm. The calcium released from a cluster of IP_3Rs or RyRs generates localized Ca^{2+} signaling events, i.e. puffs or sparks respectively [5,7]. The clustered channels will show strong stochastic dynamics due to the random opening and closing of channels, resulting in stochastic puffs with a broad range of distributions of amplitude, lifetime and inter-puff interval [8,9].

Complex intracellular Ca^{2+} signals in the presence of noise have been investigated experimentally and numerically [10–16]. Consequences of the discreteness of the release clusters for Ca^{2+} wave formation have been explored [17,18]. It is a recent interest to study how a periodic intracellular Ca^{2+} signal can be generated with a clustered channel distribution and stochastic dynamics [17–21]. It is widely known that dynamical noise can be used to enhance or induce periodicity in nonlinear systems through mechanisms such as stochastic resonance [22–26] or coherence resonance [26–29]. It has been suggested that the calcium system may use stochastic resonance dynamics to improve its signal periodicity or coherence [11,14,30]. In Ref. [30] Shuai and Jung showed that the IP_3R channels in a small cluster can increase the sensitivity of the

* Corresponding author. Tel.: +86 592 218 2575; fax: +86 592 218 9426.
E-mail address: jianweishuai@xmu.edu.cn (J. Shuai).

0378-4371/$ – see front matter
doi:10.1016/j.physa.2010.11.036

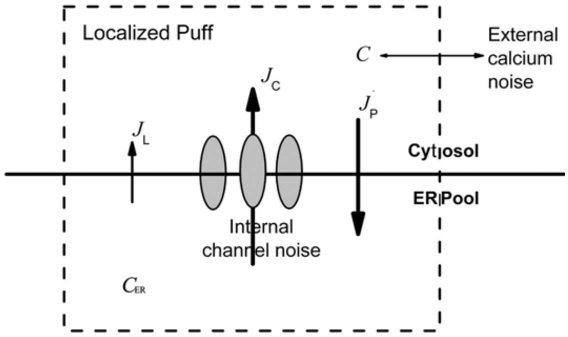

Fig. 1. The schematic diagram for the puff model. In the model, the external calcium noise represents the diffusing fluctuation between puff and environmental cytosol, and the internal channel noise is due to the stochastic channel dynamics.

calcium response allowing for coherent calcium responses to weak stimuli. According to this investigation, there exists an optimal number of IP_3Rs constituting a cluster at which the periodicity or coherence of the stochastic Ca^{2+} signal is maximized.

The activity of local enzymes or proteins may be modified by the localized calcium puffs which are released from the nearby clustered IP_3R channels. The cellular information can be encoded in the oscillatory frequency of calcium concentration. Therefore, it is of interest to discuss how the clustered Ca^{2+} channels can generate oscillatory puffs to control the subcellular functions. As yet there have been few detailed discussions and comparisons as to what differences could be obtained for localized Ca^{2+} puffs with different sources of noise, such as external calcium fluctuation and internal channel noise. In this paper, we compare the coherent calcium puff signals at weak stimulus, driven either by the intrinsic channel noise or by the environmental calcium noise. We show that, although the channel noise and the calcium noise both can show coherence resonance behavior, a surprising result is that coherent Ca^{2+} puffs with enhanced periodicity can be achieved with calcium noise more easily than with channel noise.

2. Li–Rinzel model

In this paper the simple two-variable Li–Rinzel model [31] is used to simulate calcium puff release from small clusters of IP_3Rs [8,30]. A schematic diagram for the model is given in Fig. 1. In order to apply the Li–Rinzel model for puff simulation, the channels are assumed to be close enough so that Ca^{2+} concentration can be considered homogeneous throughout the cluster. Thus we neglect spatial aspects of the formation and collapse of localized Ca^{2+} concentration in the cluster [6,8,32–34]. The Ca^{2+} diffusion between cluster and environment is treated as the fluctuation of environmental Ca^{2+} on puff dynamics (Fig. 1). This approximation is motivated by the fact that EGTA buffer has to be added in the cell to diffusively decouple nearby clusters [5]. In our paper we only consider the situation with weak IP_3 stimulation, which typically generate localized puff releases rather than the global waves in experiment [5]. The stochastic channel dynamics are simulated by the Langevin approach as suggested in Ref. [8,30].

According to the Li–Rinzel model [31], the IP_3R channel is modeled by three identical subunits that each have three binding sites: one site for the inositol 1,4,5-triphosphate (IP_3) messenger (m-gate), one activating site (n-gate) for Ca^{2+} and one inactivating site (h-gate) for Ca^{2+}. In order for a channel to be open to conduct Ca^{2+}, only the IP_3 and the activating Ca^{2+} binding site need to be occupied. The entire IP_3R is conducting if three subunits are conducting. In the Li–Rinzel model, the gating variables m and n have been replaced by their quasi equilibrium values m_∞ and n_∞ due to their fast kinetics. If we do not consider any noise, the calcium signaling model is given by Ref. [31].

$$\begin{aligned} \frac{\mathrm{d}C}{\mathrm{d}t} &= J_C - J_P + J_L \\ \frac{\mathrm{d}h}{\mathrm{d}t} &= \alpha(1-h) - \beta h \end{aligned} \tag{1}$$

with

$$\begin{aligned} J_C &= c_1 v_C m_\infty^3 n_\infty^3 h^3 (C_{\mathrm{ER}} - C) \\ J_P &= v_P \frac{C^2}{k^2 + C^2} \\ J_L &= v_L (C_{\mathrm{ER}} - C). \end{aligned} \tag{2}$$

Here, C denotes the localized Ca^{2+} concentration released from a cluster of channels, C_{ER} the Ca^{2+} concentration in the ER, and h the slow inactivation variable. J_C denotes Ca^{2+} efflux from intracellular stores through clustered IP_3R channels, J_P the ATP-dependent Ca^{2+} flux from the intracellular space back to the stores, and J_L the leakage flux (Fig. 1).

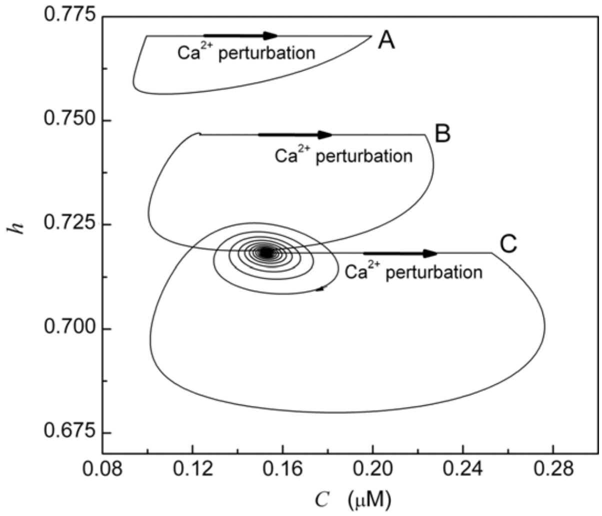

Fig. 2. Transient trajectory of the deterministic model in the C–h plane. Perturbation A is at $p = 0.25$ μM, B at $p = 0.3$ μM and C at $p = 0.34$ μM. The arrow represents the calcium perturbation with $\delta C = 0.1$ μM.

The slow Ca^{2+} inactivation process depends on both the concentration of IP_3 and Ca^{2+} via the rate constants

$$\alpha = ad_2\frac{p+d_1}{p+d_3} \qquad (3)$$
$$\beta = aC$$

in which p denotes the concentration of IP_3 messenger. The quasi-equilibrium states of m and n are

$$m_\infty = \frac{p}{p+d_m} \qquad (4)$$
$$n_\infty = \frac{C}{C+d_n}.$$

According to Ref. [31], the model parameters are $c_1 = 0.185$, $v_C = 6\ \mathrm{s}^{-1}$, $v_L = 0.11\ \mathrm{s}^{-1}$, $v_P = 0.9\ \mu\mathrm{M\ s}^{-1}$, $k_3 = 0.1\ \mu\mathrm{M}$, $d_1 = 0.13\ \mu\mathrm{M}$, $d_2 = 1.049\ \mu\mathrm{M}$, $d_3 = 0.9434\ \mu\mathrm{M}$, $d_5 = 0.08234\ \mu\mathrm{M}$, and $a_2 = 0.2\ \mu\mathrm{M}^{-1}\ \mathrm{s}^{-1}$. The total amount of Ca^{2+} is conserved via the Ca^{2+} concentration in ER with $C + c_1C_{\mathrm{ER}} = c_0$ with $c_0 = 2.0$ μM. The concentration p is a control parameter.

3. Transient trajectory at subthreshold IP_3 concentration

First we simply discuss some properties of the deterministic Li–Rinzel model. The bifurcation diagram of the deterministic Li–Rinzel model shows an oscillation behavior at $0.354 < p < 0.642$ μM [31]. Fixed points can be obtained for $p < 0.354$ μM. Depending on the value of p, the fixed points have different properties. For example, the fixed point is a node with two negative eigenvalues at $p = 0.25$ μM. At $p = 0.30$ μM the fixed point has two eigenvalues of $-0.32 \pm 0.39\sqrt{-1}$. Due to the large damping term of -0.32, the transient trajectory hardly shows an oscillating transient when the system starts from any other point. However, for the fixed point at $p = 0.34$ μM, the two eigenvalues are $-0.06 \pm 0.5\sqrt{-1}$ and a spiral transient trajectory appears. This can be seen clearly in Fig. 2, in which the transient trajectories of the model are plotted for a calcium perturbation of $\delta C = 0.1$ μM beyond its steady calcium concentration.

With a subthreshold IP_3 concentration (i.e. $p < 0.354$ μM), the deterministic model gives a fixed point and does not permit calcium signaling. If the system is driven by noise at a subthreshold value of $p = 0.34$ μM, which is near the threshold, the system will typically show a spiral transient oscillation (Fig. 2), giving the behavior of coherence resonance. However, in the paper we show that the coherence resonance can be also observed for a system far below the bifurcation point, even at $p = 0.30$ or 0.25 μM, where the transient trajectory is largely damped (Fig. 2). We also discuss how the different sources of noise can cause different behaviors of coherence resonance for the puff system.

4. Coherent calcium puff signals with external calcium noise

The calcium puffs are always coupled to the environmental cytosol by diffusion, which is simply treated as the external calcium fluctuation in the model. Thus we consider the following Langevin equation

$$\frac{\mathrm{d}C}{\mathrm{d}t} = J_C - J_P + J_L + D_C\xi(t) \qquad (5)$$

where the constant parameter D_C represents the noise variance of the environmental calcium fluctuation.

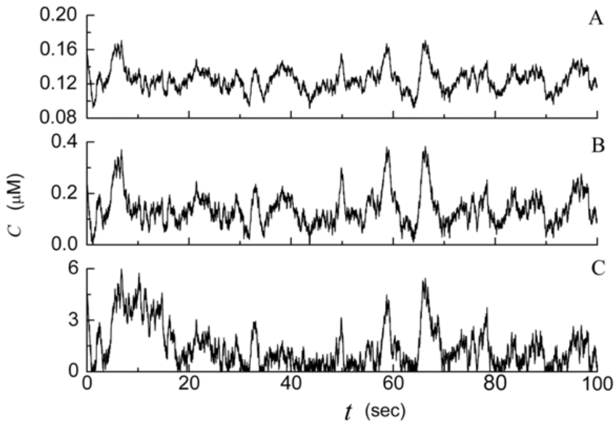

Fig. 3. Stochastic trajectories of the Ca^{2+} signal at $p = 0.30$ μM with noise strength $D_C = 0.01$ (A), 0.05 (B) and 1.0 (C).

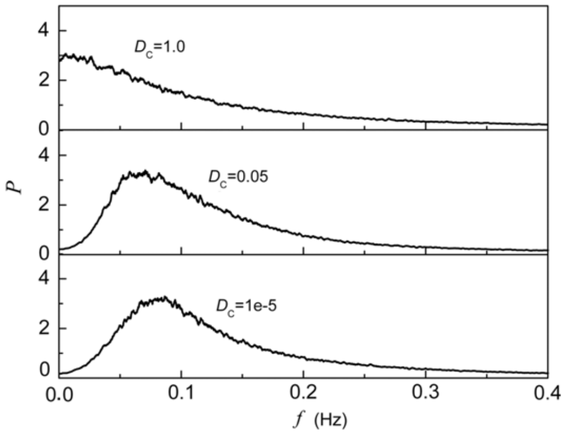

Fig. 4. The power spectra P of the Ca^{2+} signal versus frequency f of the puff model disturbed by Ca^{2+} noise at $p = 0.3$ μM with noise strength $D_C = 1$, 0.05 and 10^{-5}.

Examples of stochastic calcium trajectories are given in Fig. 3 at $p = 0.30$ μM with $D_C = 0.01$, 0.05 and 1. Visually, changes in the temporal regularity of the calcium signals in Fig. 3 are not apparent for varying D_C. However, there are signatures of such a change. To characterize the degree of the temporal regularity of the calcium signals, we compute the power spectrum.

Because we want to discuss the periodicity of the trajectory, the power spectrum calculated here is renormalized to 1. To reduce statistical fluctuations due to the finite time-interval of recording, at each noise strength 100 power spectra are calculated and averaged to get an averaged power spectrum. Then the adjacent averaging process is applied to get a smoother power spectrum. The normalized power spectra of Ca^{2+} signals are given in Fig. 4 at $p = 0.3$ μM with $D_C = 1$, 0.05 and 10^{-5}. For large D_C, the power spectrum does not exhibit a typical peak and thus the release of Ca^{2+} is dominated by stochastic events. However, with a small noise, a peak in the power spectrum indicates an increased periodicity in the calcium signals.

The periodicity of the calcium signals can be described by the elevation of the peak ΔP [30], i.e.

$$\Delta P = P_{\mathrm{Peak}} - P(0). \tag{6}$$

The periodicity index ΔP as a function of D_C is shown in Fig. 5(A) for $p = 0.3$ and 0.25 μM. The elevation of the power spectrum goes through a maximum at $D_C = 0.02$ for $p = 0.3$ μM and at $D_C = 0.05$ for $p = 0.25$ μM. Thus, the overall coherence of the Ca^{2+} signal exhibits a maximum at different noise strength that depends on the concentration of IP_3. The simulation results also show that a peak can be observed with a very small noise, even at $D_C = 10^{-6}$. This is a surprising result, suggesting that the enhanced periodicity of calcium signals can be achieved easily even with small calcium noise.

Actually the calcium fluctuation amplitude decreases with a decrease of the noise strength. A very small noise typically generates a very weak fluctuation of calcium around its fixed point. Thus a better parameter to characterize the noise-induced coherent signal is to consider the combination of the oscillating amplitude and periodicity of the trajectory. Accordingly, we define a signal index, which is given as

$$\Gamma = \Delta P \cdot H \tag{7}$$

with the parameter H the standard deviation of the calcium fluctuation around its mean value. The signal index as a function of D_C is shown in Fig. 5(B). One can see that a large signal index is found at $D_C = 0.1$ with $p = 0.3$ μM and at $D_C = 0.2$ with $p = 0.25$ μM. With small D_C, the calcium fluctuation decreases, resulting in a small signal index.

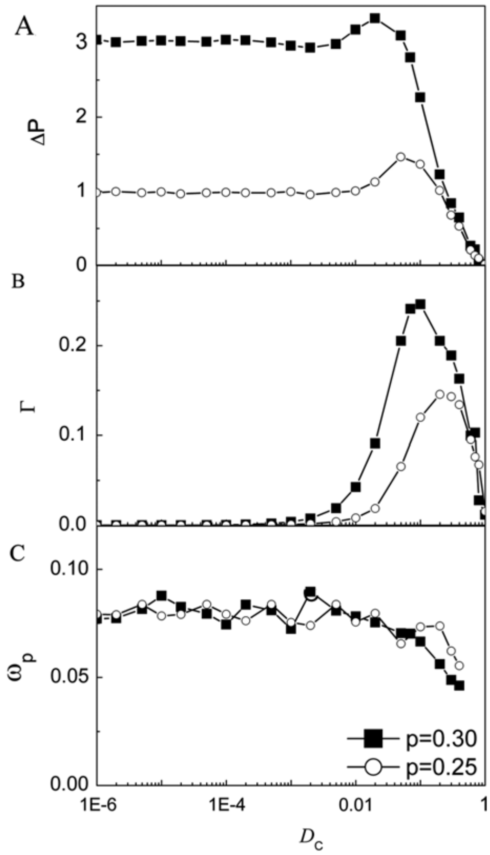

Fig. 5. The coherent calcium puffs driven by calcium noise. (A) The peak elevation ΔP, (B) the signal index Γ, and (C) the peak frequency ω_P of the power spectrum of the calcium signal versus D_C at $p = 0.3$ μM (squares) and $p = 0.25$ μM (circles).

Another parameter related to the periodicity of calcium signal is the peak frequency of spectrum. The plot of peak frequency ω_P against D_C is given in Fig. 5(C). At small D_C, the frequency ω_P is almost fixed at 0.08 Hz for both $p = 0.3$ and 0.25 μM. However, with the increase of D_C beyond $D_C = 0.005$, the peak frequency decreases.

5. Coherent calcium puff signals with internal channel noise

A cluster of IP_3R channels exhibits stochastic channel dynamics. For the puff simulation with the Li–Rinzel model, the stochastic dynamics of opening and closing of channels were considered due to the stochastic binding and unbinding dynamics of Ca^{2+} and IP_3 on the channel [8,30]. In fact, there are various types of noise occurring in cells that can affect the channel dynamics. For example, due to thermal fluctuation, the conformations of IP_3Rs can change randomly, resulting in the fluctuation of binding/unbinding rates for Ca^{2+} ions and IP_3 messengers. Thus here we consider a general noise on the channel dynamics, given as

$$\frac{dh}{dt} = \alpha(1-h) - \beta h + D_h \xi(t) \tag{8}$$

where D_h is the deviation of Gaussian white noise related to stochastic channel dynamics. Thus the channel noise is a type of internal noise for puff dynamics.

In order to discuss the periodicity of the trajectory disturbed by channel noise, the normalized power spectra of Ca^{2+} signals are calculated. Fig. 6 shows three spectra at $p = 0.3$ μM with $D_h = 1$, 0.01 and 10^{-4}. For large and small D_h, the power spectra do not exhibit a typical peak and thus the release of Ca^{2+} is dominated by stochastic events. However, with suitable noise, a peak in the power spectrum indicates an increased periodicity in calcium signals.

The peak elevation of power spectrum ΔP as a function of D_h is shown in Fig. 7(A) for $p = 0.3$ and 0.25 μM. Simulation results indicate that the calcium noise (i.e. Eq. (5)) and channel noise (i.e. Eq. (8)) have different effects on the periodicity of the calcium signals. With the channel noise, a large ΔP can be obtained for D_h in the region from 0.002 to 0.05. Such a noise can be caused by the stochastic channel open–closing dynamics for a cluster of several tens of IP_3R channels, which is about the cluster size observed in cells for puff release [30]. As a comparison between Figs. 7(A) and 5(A), channel noise and calcium noise show quite different coherent behavior on Ca^{2+} signals.

The signal index and the peak frequency ω_P as a function of D_h are shown in Fig. 7(B) and (C). One can see that a large signal index is found at $D_C = 0.02$ with $p = 0.3$ μM and at $D_C = 0.03$ with $p = 0.25$ μM. With small D_C, the calcium

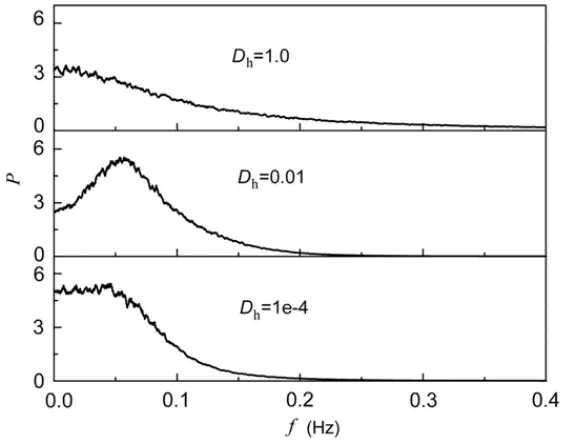

Fig. 6. The power spectra P of the Ca^{2+} signal versus frequency f of the puff model disturbed by channel noise at $p = 0.3$ μM with noise strength $D_h = 1$, 0.01 and 10^{-4}.

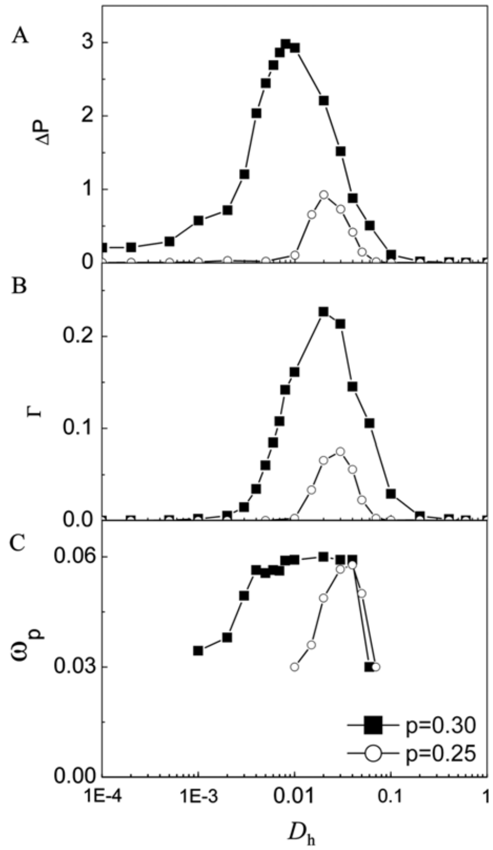

Fig. 7. The coherent calcium puffs driven by channel noise. (A) The peak elevation ΔP, (B) the signal index Γ, and (C) the peak frequency ω_P of the power spectrum of the calcium signal versus D_h at $p = 0.3$ μM (squares) and $p = 0.25$ μM (circles).

fluctuation decreases, resulting in a small signal index. The frequency ω_P at the power peak is in the range from 0.03 to 0.06 Hz for both $p = 0.3$ and 0.25 μM. As a comparison between Figs. 5 and 7, one can see that the maximal signal index and the peak frequency are achieved at different noise strength with channel noise or calcium noise.

6. Conclusion and discussion

In this paper we have studied the coherence resonance of calcium puffs released from intracellular pools through a cluster of IP_3R channels. We applied the Li–Rinzel model as an example for discussion, because it is simple and computationally efficient. We expect that other mathematical IP_3R–Ca^{2+} models of excitable structures would yield similar results. We showed that different sources of noise, either an external noise or an internal noise, can generate different coherent puff signals. A surprising result is that the calcium signals show an enhanced periodicity for a very large range of calcium noise strength. It means that the enhanced periodicity of calcium signals can be achieved more easily by external calcium noise than internal channel noise.

An interesting question is why the calcium noise can be more effective than the channel noise in enhancing the periodicity of calcium puff signals. A possible mechanism may involve the shift of nullclines and the closeness of the Hopf instability. As indicated in Ref. [31], the variables C and h in the Li–Rinzel model are a voltage-like fast activator and a recovery-like slow inhibitor respectively. Thus our simulation results imply that a perturbation in the fast calcium variable can easily shift its nullcline toward the Hopf instability, whereas a perturbation in the slow inhibitor will slowly shift its nullcline toward the Hopf instability. However, this argument remains to be investigated in the future using detailed phase space analysis.

Although a small calcium noise can generate a periodicity-enhanced calcium signal, its fluctuation amplitude is normally small and is hard to detect biologically. Thus, a better parameter to characterize the noise-induced coherent signal is to consider the signal index, which is a combination of the oscillating amplitude and periodicity of the trajectory. The Li–Rinzel model shows a similar coherence resonance with calcium noise and channel noise.

It has been suggested that the cellular information is mainly encoded in the frequency of calcium signals [1–4]. The gene or enzyme activations are modulated by the frequency of calcium oscillations. In this paper we show that an enhanced periodicity of calcium puff signal can be obtained with external calcium noise or internal channel noise. This result may find interesting applications in calcium signaling for localized cellular function. We also suspect that similar behavior can be observed in other noise-driven nonlinear systems.

Acknowledgement

J.S. would like to acknowledge the support of this work by the National Science Foundation of China under Grants 10775114 and 30970970.

References

[1] M.J. Berridge, M.D. Bootman, P. Lipp, Nature 395 (1998) 645–648.
[2] R.E. Dolmetsch, K.L. Xu, R.S. Lewis, Nature 392 (1998) 933–936.
[3] W.H. Li, J. Llopis, M. Whitney, G. Zlokarnik, R.Y. Tsien, Nature 392 (1998) 936–941.
[4] P. De Koninck, H. Schulman, Science 279 (1998) 227–230.
[5] X.P. Sun, N. Callamaras, J.S. Marchant, I. Parker, J. Physiol. 509 (Pt. 1) (1998) 67–80.
[6] S. Swillens, G. Dupont, L. Combettes, P. Champeil, Proc. Natl. Acad. Sci. USA 96 (1999) 13750–13755.
[7] H.P. Cheng, W.J. Lederer, Physiol. Rev. 88 (2008) 1491–1545.
[8] J.W. Shuai, P. Jung, Biophys. J. 83 (2002) 87–97.
[9] G. Ullah, P. Jung, Biophys. J. 90 (2006) 3485–3495.
[10] Z.H. Hou, J.Q. Zhang, H.W. Xin, Phys. Rev. E 74 (2006) 031901 1-5.
[11] A.K. Nchange, W.D. Kepseu, P. Woafo, Physica A 387 (2008) 2519–2525.
[12] M. Perc, M. Gosak, M. Marhl, Chem. Phys. Lett. 437 (2007) 143–147.
[13] M. Perc, A.K. Green, C.J. Dixon, M. Marhl, Biophys. Chem. 132 (2008) 33–38.
[14] M. Perc, M. Marhl, Physica A 332 (2004) 123–140.
[15] M. Perc, M. Gosak, M. Marhl, Chem. Phys. Lett. 421 (2006) 106–110.
[16] M. Falcke, Chaos 19 (2009) 037101 1-3.
[17] S.P. Dawson, J. Keizer, J.E. Pearson, Proc. Natl. Acad. Sci. USA 96 (1999) 6060–6063.
[18] J.W. Shuai, P. Jung, Proc. Natl. Acad. Sci. USA 100 (2003) 506–510.
[19] J.W. Shuai, P. Jung, Phys. Rev. E 67 (2003) 031905 1-8.
[20] A. Skupin, H. Kettenmann, U. Winkler, M. Wartenberg, H. Sauer, S.C. Tovey, C.W. Taylor, M. Falcke, Biophys. J. 94 (2008) 2404–2411.
[21] R. Thul, G.D. Smith, S. Coombes, J. Math. Biol. 56 (2008) 435–463.
[22] J.J. Collins, T.T. Imhoff, P. Grigg, J. Neurophysiol. 76 (1996) 642–645.
[23] L. Gammaitoni, P. Hanggi, P. Jung, F. Marchesoni, Rev. Modern Phys. 70 (1998) 223–287.
[24] L. Gammaitoni, P. Hanggi, P. Jung, F. Marchesoni, Eur. Phys. J. B 69 (2009) 1–3.
[25] A.A. Priplata, J.B. Niemi, J.D. Harry, L.A. Lipsitz, J.J. Collins, Lancet 362 (2003) 1123–1124.
[26] B. Lindner, J. García-Ojalvo, A. Neiman, L. Schimansky-Geier, Phys. Rep. 392 (2004) 321–424.
[27] A.S. Pikovsky, J. Kurths, Phys. Rev. Lett. 78 (1997) 775–778.
[28] J.R. Pradines, G.V. Osipov, J.J. Collins, Phys. Rev. E 60 (1999) 6407–6410.
[29] M. Perc, Chem. Phys. Lett. 410 (2005) 49–53.
[30] J.W. Shuai, P. Jung, Phys. Rev. Lett. 88 (2002) 68102 1-4.
[31] Y.X. Li, J. Rinzel, J. Theoret. Biol. 166 (1994) 461–473.
[32] S. Rudiger, J.W. Shuai, I.M. Sokolov, Phys. Rev. Lett. 105 (2010) 048103 1-4.
[33] J. Shuai, R. Sheng, P. Jung, Phys. Rev. E 81 (2010) 051913 1-7.
[34] S. Rudiger, C. Nagaiah, G. Warnecke, J.W. Shuai, Biophys. J. 99 (2010) 3–12.